Annu. Rev. Phys. Chem. 1993. 44: 369–95

HYDRATION FORCES

S. Leikin, V. A. Parsegian, and D. C. Rau

Division of Computer Research and Technology, and National Institute of Diabetes and Digestive and Kidney Diseases, National Institutes of Health, Bethesda, Maryland 20892

R. P. Rand

Department of Biological Sciences, Brock University, St. Catharines, Ontario, Canada, L2S 3A1

KEY WORDS: molecular interactions, molecular solvation, surface forces, water structure

INTRODUCTION

For generations, the central paradigm of colloid science held that electrostatic and electrodynamic (van der Waals) forces were the principal determinants of colloidal systems (1, 2). So firm was the grip of this belief that the paradigm has reflexively been carried over to apply to macromolecular interactions, especially to the interaction of biological membranes or macromolecules (3).

The trouble is this assumption is often wrong. Just when membranes or molecules are in strong and morphologically significant interaction, within the last 10–20 Ångstroms of separation the whole thing begins to break down. One must return to an earlier idea (4–7) that the interaction of water-soluble bodies is best seen as their interaction with water itself. In clinging to the solvent, they consequently repel each other, except in those peculiar and intentional circumstances when the match between molecular surfaces is stronger than with the host solvent itself.

Despite its categorical tone, our title is intended to recognize a general kind of behavior, recognition of a ubiquitous feature of forces that have now been directly measured among all classes of lipid membranes, biological macromolecules, and some colloidal systems, an unexpected exponentially varying force whose integrated strength necessarily comes to

0066–426X/93/1101–0369$05.00

equal the enormous energies of solvation itself. The concept, "hydration forces," did not come easily. Only when direct, systematic measurements revealed surprisingly strong exponentially varying repulsion between neutral lipid bilayer membranes in distilled water as they entered the last few nanometers of separation did one realize that the old ideas didn't work (8). Then, as the same kinds of forces appeared between materials as diverse as minerals and glasses (9), natural and synthetic lipids (10), DNA double helices (11), stiff polysaccharides (12), and proteins (13), new rules for thinking about molecular interaction impressed themselves on us.

Still, our understanding is only empirical. The underlying properties of the solvent still elude us. Interpretations alternative or supplementary to solvation must be continually recognized. Indeed there are many, often mutually exclusive, hypotheses. The choice between them can be subjective and selective of the particular data to be addressed. Here, we have tried to be fair to all points of view without compromising our own considered conclusions and to give enough information to allow others to think clearly about the sources and consequences of these newly delineated interactions.

We begin with a brief citation and appraisal of several force-measurement methods, then extensively review systematically measured forces involving well-defined materials. Several themes emerge from these measurements—empirical rules that suggest the theoretical speculations presented next.

Paradoxically, the most important part of the subject cannot yet be properly reviewed. Newly recognized forces both between and within large molecules or membranes must change our ideas about how these materials perform. Unexpected interactions require new theories of forces whose consideration has hardly begun. This review ends with questions and suggestions for new strategies for learning.

MEASURING INTERMOLECULAR FORCES

Experimental Techniques

Hydration forces have been directly measured or inferred by using several different methods. We outline here the features pertinent to comparing results from the most widely used techniques. The Osmotic Stress (OS) method (8, 11, 14) has been used for measuring forces between lipid bilayers and linear macromolecules in ordered macromolecular assemblies. A sample is equilibrated with a reservoir solution containing water and other small solutes, which can freely exchange with the ordered phase, as well as a stressing polymer that is excluded from it. The polymer concentration controls the osmotic stress or pressure acting on the bilayer or macromolecular phase. The spacing between bilayers or macro-

molecules is measured by using X-ray diffraction (10, 15). The OS experiment is thermodynamically equivalent to a closely related technique, in which an actual pressure is applied on the ordered phase with a semipermeable piston that passes only water and small solutes (14, 16). Similar preparations, which lack the ability to control the activity of salt or other small solutes, can be made by exposing the ordered sample to vapors of controlled relative humidity (14, 17–19).

Several mechanical, force-balance methods have been developed for measuring forces between curved solid surfaces (9, 20–26). Probably the most widely used of these mechanical devices is the surface force apparatus (SFA) (9, 20, 24), although use of the atomic force microscope (AFM) has increased recently (25, 26). In the SFA method, thin, transparent solid films (usually mica sheets) are glued onto crossed cylindrical glass surfaces. The force between these glued surfaces is applied from the back by a cantilever spring system. The separation is measured by means of optical interference fringes set up between silvered backings on the films. The SFA method is often used for measuring forces between surfactant, lipid, or other molecular monolayers that are coated onto mica sheets (9).

This technique appears to be more versatile than OS for measuring very long-range interactions out to spacings of thousands of Ångstroms. The applicability of force-balance techniques to interactions at close spacings is, however, limited. The geometry of curved surfaces emphasizes longer-range van der Waals and electrostatic double layer forces at the expense of the shorter-range hydration force (27, 28). In addition, these surfaces are deformed at high pressures (29–31), distance measurement is less accurate than that by using X-ray diffraction, and surface interaction with glue leaching into solution or with even trace amounts of water contaminants might greatly affect forces at close separation (20, 32–34). In several overlapping experiments on lipid bilayers, the agreement between SFA and OS was very good, when results were carefully compared (27, 35). However, the possibilities for direct comparison are very limited, given the difference in the optimal range of measurement and the differences in the structure, stability, and ordering between lipid bilayers adsorbed on mica and bilayers assembled in solution (36). We believe that SFA and OS should be viewed as complementary methods rather than competing techniques.

Lipid Bilayers

Figure 1 illustrates force-distance curves measured by OS for several different lipid bilayers in water. From their equilibrium spacing with no applied stress, net neutral, zwitterionic lipid bilayers repel each other with exponentially increasing force P over the last few nanometers of

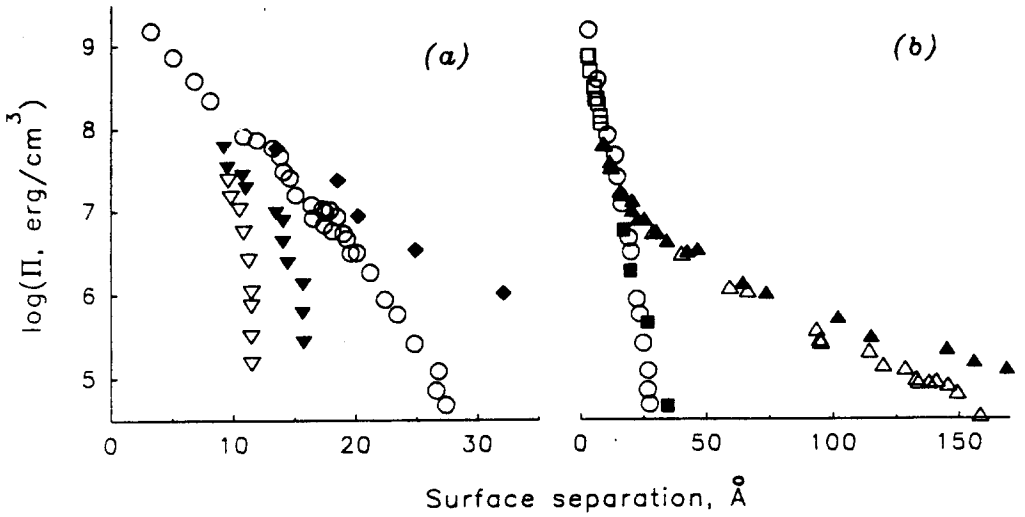

Figure 1 Typical osmotic stress ($-\Pi\cdot$) vs surface separation curves for different lipid bilayers. Zwitterionic lipid bilayers in distilled water: (○) egg phosphatidylcholine (egg PC), (▽) palmitoyloleoylphosphatidylethanolamine (POPE), (▼) phosphatidylethanolamine trans-phosphatidylated onto egg PC chains (egg PEt). Charged double-chain surfactants: (◆) didodecylphosphate (DDP) in 0.5 M tetramethylammonium chloride (TMACl), dihexadecyldimethylammonium acetate (DHDAA) in water vapor (□) and various concentrations of sodium acetate [0.005 M (▲), 0.015 M (△), 0.5 M (■)]. Osmotic stress and repulsive force/area are equivalent for planar bilayers ($\Pi = P(d_w)$).

In *b*, DHDAA force curves at low salt concentration and large spacings show electrostatic double layer repulsion. At smaller spacings or at high salt concentration, both DDP and DHDAA reveal hydration forces, which no longer depend on the solution ionic strength. While TMA^+ adsorption on DDP^- bilayers appears to be weak, acetate counterions are strongly bound to DHDAA, leaving only 1/6 the expected surface-charge density (28). Data for net neutral egg PC shown together with DHDAA data demonstrate almost identical salt-independent hydration forces for these two lipids.

Table 1 gives the hydration force parameters for the lipids shown in this figure. The reliability of the extracted numbers depends on the range of distances and pressures over which the force can be measured. While the reliability is high for egg PC and DHDAA as well as for several other lipids not shown here, it is much lower for POPE. These numbers can also slightly vary depending on the method used for extracting the distance between the bilayers from multilamellar repeat spacing (10). The data shown in this figure have been obtained using the traditional gravimetric procedure of Luzatti (37). The hydration force parameters can be determined more accurately (10, 38) combining the gravimetric or electron density (15) procedures with independent, sensitive measurements (39) of bilayer lateral compressibility. In Table 1 we give the adjusted force parameters when compressibility data are available.

separation, d_w,

$$P(d_w) = P_o \exp(-d_w/\lambda), \qquad 1.$$

with decay lengths, λ, ranging between 1–3 Ångstroms (8, 10, 15, 40–42). This force depends negligibly on the ionic strength and composition of the bathing solution (42–44). A similar force is observed between totally

uncharged mono- and diglyceride bilayers (10, 45). Charged lipids show an electrostatic, double-layer repulsion with the expected force dependence on bilayer charge and electrolyte concentration, but only at separations larger than 20–30 Å (28, 35, 36, 46–50). At closer distances, this electrostatic force is overwhelmed by a salt-independent, exponential "hydration" repulsion, similar to the neutral lipid forces (28, 35, 46, 50).

One can get some idea of the strength of hydration repulsion by examining the cost of removing all water separating lipid bilayers. Specifically integrating the observed force to obtain the work needed for bringing egg phosphatidylcholine bilayers to contact gives an energy of 100 erg/cm^2 or $\sim$5 kcal/mol of lipid molecules (10). For comparison, ATP hydrolysis yields 7.3 kcal/mol; H-bonds are $\sim$5 kcal/mol.

Exponential hydration-like repulsion has been also measured in several polar, nonaqueous solvents (51, 52). The decay length seems to scale with the size of the solvent molecule, suggesting a direct connection between the solvent and the force (52).

The forces shown in Figure 1 are qualitatively similar in all cases. Both the force amplitude P_o and the decay length λ, however, depend on the nature of the lipid. Table 1 summarizes the exponential force parameters for the lipid bilayers shown in Figure 1. The most dramatic example of this sensitivity appears in the comparison of force curves for phosphatidylethanolamine (PE) and phosphatidylcholine (PC) bilayers. The change in lipid polar head from an amine group in PE to a trimethylamine group in PC results in the increase in the equilibrium separation at zero applied stress from $\sim$12 Å to 25–30 Å, an increase in the apparent decay length λ from $\sim$1 to $\sim$2.5 Å and a decrease in P_o from $\sim 10^{12}$ to $\sim 10^{10}$ dyn/cm (10, 38). Successive methylation of egg PE shows that the first substituted methyl group causes the largest change in the force (38).

An even larger decay length of $\sim$5 Å, independent of ionic strength, is observed for charged didodecylphosphate (DDP) bilayers with tetramethylammonium (TMA^+) counterions in solution (see Figure 1). The overlapping of force magnitudes for TMA-DDP and PC bilayers at spacings less than $\sim$20 Å suggests that at close distances the force is not greatly affected by whether the tetraalkylamine is free in solution, as with TMA-DDP, or covalently bound in the polar head group, as with PC.

A correlation between bilayer P_o and monolayer dipole potential has been observed for several lipids, suggesting that some kind of surface "polarity" plays an important role in the interaction (50, 52, 57–62). The dipole potential by itself, nevertheless, is not sufficient to explain all lipid data. For example, ether lipids that lack the fatty acid carbonyl group show a twofold smaller dipole potential than do the equivalent ester lipids, but within experimental accuracy bilayer forces seem unaffected (63).

Table 1 Measured and predicted hydration force parameters for different materials

Material (references)	Measured force parameters		Mean field model prediction
	log P_o (erg/cm^3)	λ_{exp} (Å)	λ_{theor} (Å)
Materials with similar λ			
TMA^+-DDP	9.1	4.5	
TMA^+-DNA (53)	8.9	4.0 (4–5)[a]	
Na^+-DNA (11, 53)	8.7	3.3 (4–5)[a]	4–5
Na^+-Xanthan (12)	8.3	3.4 (4–5)[a]	
Schizophyllan (12)	7.3	4.0	
Silica (21, 22, 54)		5–10	
Materials with varying λ			
zwitterionic lipid bilayers (10)			
egg PC	10.6[b]	2.1[b]	
egg PEt	12.3[b]	1.1[b]	
POPE	12.5[b]	0.8[b]	0.7 to 2–2.5
DPPC 25°C (frozen chains)	12.3[b]	1.1[b]	
DPPC 50°C (melted chains)	11.0[b]	2.1[b]	
charged lipid bilayers			
DHDAA (28)	9.2	3.0	0.7 to 4–5
Na^+-DPPG (50)	11.9–12.2	0.7–0.8	
uncharged lipid bilayers			
DGDG (10)	10.3[b]	1.7[b]	0.7 to 4–5
Monoelaidin (45)	9.7	1.3	
counterion-condensed DNA			
Co^{3+}-DNA (55)	9.6	1.3	1.6–1.8[c]
Mn^{2+}-DNA (56)	92.	1.3	
protein			
Rat tail collagen	10.2	0.6	0.7[c]

[a] Values in parentheses are obtained by fitting the data to a cylindrically-symmetric analog of Equation 2 (55).

[b] Values adjusted for compressibility of lipid bilayers (10, 38).

[c] Values predicted for interaction between planar surfaces.

Abbreviations: TMA, tetramethylammonium; DDP, didodecylphosphate; PC, phosphatidylcholine; PE, phosphatidylethanolamine; PEt, PE transphosphatidylated onto PC chains; POPE, palmitoyloleoyl PE; DPPC, dipalmitoyl PC; DHDAA, dihexadecyldimethylammonium acetate; DPPG, dipalmitoylphosphatidylglycerol; DGDG, digalactosyldiglyceride.

Even though surface chemistry and polarity seem to be key factors in the interaction, melting of hydrocarbon chains and increases in chain length, heterogeneity, polyunsaturation, and conformational disorder often result in larger λ and stronger repulsion (10, 15, 38, 40).

Bilayers with mixed composition show several surprising features. Bilayers of PE/PC mixtures swell to a much greater extent than predicted by linear superposition of pure PE and PC data (38). PE/digalactosyldiacylglycerol (DGDG) mixtures swell significantly more than either component alone (10). Mixing PC with diacylglycerol, a lipid with no significant polar group, results in a larger λ and stronger repulsion (64; J. Bech & R. P. Rand, in preparation). Cholesterol incorporated into bilayers can cause stronger or weaker repulsion with larger or smaller λ, depending on the lipid composition and hydrocarbon chain conformation (10, 40, 59, 62). When added to egg PC bilayers, ketocholestanol, a cholesterol analogue with a large dipole moment, produces stronger repulsion without changing the decay length (61).

The limited swelling of several neutral bilayers, such as PC, can be understood as a balance between a repulsive hydration force and an attractive van der Waals interaction (65). However, an attractive force significantly stronger than a van der Waals interaction is required to explain the very limited swelling of bilayers like PE (38).

DNA, Polysaccharides, and Proteins

Although they are often neglected, hydration forces occur with materials other than lipid bilayers. Figure 2 demonstrates the similarity of force curves measured using OS for highly charged lipid bilayers of DDP (Y. Fang & R. P. Rand, in preparation); for highly charged DNA (11, 53, 66); for xanthan, a moderately charged polysaccharide (12); and for schizophyllan, an uncharged carbohydrate (12).

In contrast to the data for lipids, these stiff helical macromolecules exhibit remarkably little variation in the decay length λ (Table 1). Force amplitudes P_o, however, are strongly affected by the nature of the surface and vary by almost two orders of magnitude. No dependence of the force on salt concentration is observed at spacings less than 10–20 Å. DNA force amplitudes, however, depend on the bound counterion species (11, 66). Force curves for xanthan, with little or no observed ion binding, are independent of both salt concentration and counterion species (12).

The force-distance curves for lipid bilayers of DDP and for DNA, both in TMA^+, are well suited for numerical comparison, because both surfaces are composed of polar phosphate groups balanced by solution TMA^+ cations. Figure 2 shows the excellent agreement between the force curves at spacings smaller than 10–15 Å, once DNA data are rescaled to account for the difference in phosphate surface density. At larger spacings, thermal undulations enhance the force between flexible DNA molecules (53),

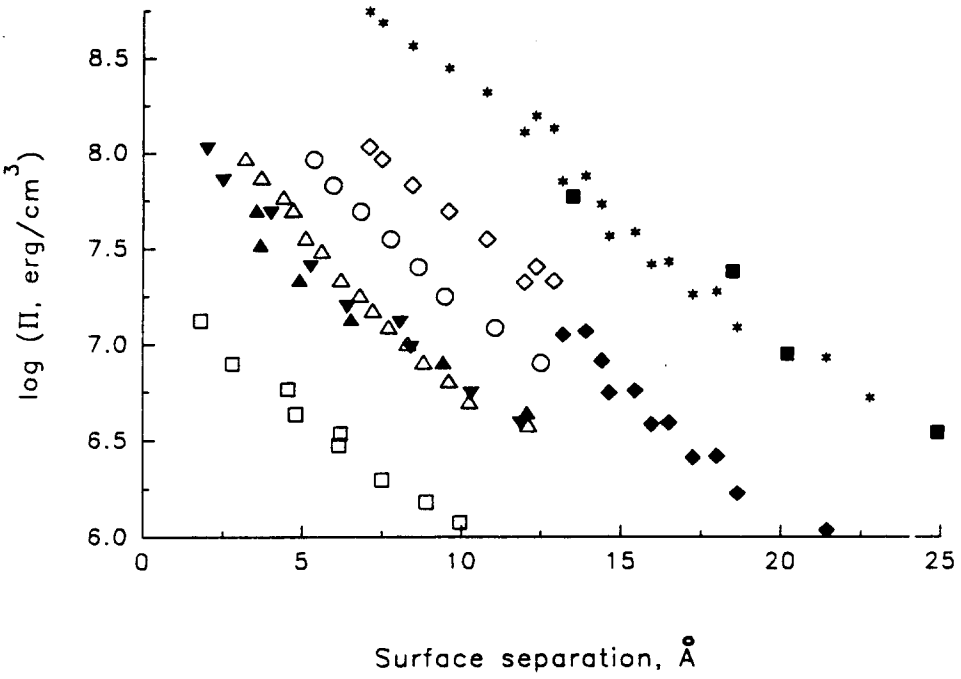

Figure 2 Osmotic pressure vs surface separation curves are shown for arrays of several stiff, helical macromolecules. The intermolecular force/unit surface area. $-\Pi'$, acting on rod-like molecules packed in a hexagonal lattice can be estimated from the osmotic pressure, Π, as $P \approx (D_{int}/D_0)\Pi$, where D_{int} is the interhelical separation and D_0 is the cylinder diameter (11, 55). Data are shown for schizophyllan (□) in water; for xanthan in 0.8 M NaCl (▼) and in 10 mM $MgCl_2$ (▲); for DNA in 10 mM $MgCl_2$ (△), in 0.4 M NaCl (○), and in 0.4 M TMACl at spacings less than about 13 Å (◇) and at larger spacings (◆) corrected for molecular undulation (R. Podgornik, D. C. Rau & V. A. Parsegian, in preparation). Table 1 summarizes the apparent exponential force parameters. The data for the lipid bilayers of DDP in 0.5 M TMACl (■) are compared with the force data (*) for DNA in 0.4 M TMACl (both directly measured and undulation corrected), adjusted for the difference in surface area per phosphate between DNA (105 Å^2) and DDP (~55 Å^2).

whereas for TMA^+-DDP this undulatory contribution is still negligible (Y. Fang & R. P. Rand, in preparation). However, after corrections for undulatory forces are included (R. Podgornik, D. C. Rau & V. A. Parsegian, in preparation), the renormalized force for TMA^+-DNA again becomes virtually identical to TMA^+-DDP data.

Most mono- and divalent ions do not prevent indefinite swelling of DNA. Sufficient concentrations of some transition-metal ions and almost all tri- and multivalent cations, however, cause spontaneous DNA assembly into ordered arrays of helices with a surface separation of 7–12 Å, depending on counterion species but not on its concentration over the critical level necessary for precipitation (55, 56). With some divalent metal ions, notably Mn^{2+} and Cd^{2+}, spontaneous assembly is favored at higher temperatures (56).

Temperature-dependent assembly, closely resembling precipitation of DNA by Mn^{2+}, is also characteristic of collagen fiber formation. Once again, collagen triple-helical surfaces are not in direct contact at their zero-stress, equilibrium spacing, but are rather separated by water.

Figure 3 illustrates the similarity of forces seen in spontaneously assembled systems with close equilibrium spacings, PE bilayers (38), counterion-condensed DNA (55, 56), and reconstituted collagen fibers at neutral pH (13). The residual repulsive forces that prevent closer approach of the surfaces all appear to vary exponentially, but with short decay lengths (Table 1). Decay lengths for the three DNA curves vary between 1.3 and 1.5 Å, rather than the 3- to 4-Å decay lengths seen in Figure 2. The decay length for collagen is about 0.6 Å. For each material, osmotic stress curves are independent of salt concentration. The spontaneous assembly of all these systems appears to require an attractive force significantly stronger than expected from van der Waals interactions. An attractive "hydration" force has been suggested as the source of this strong interaction (38, 55).

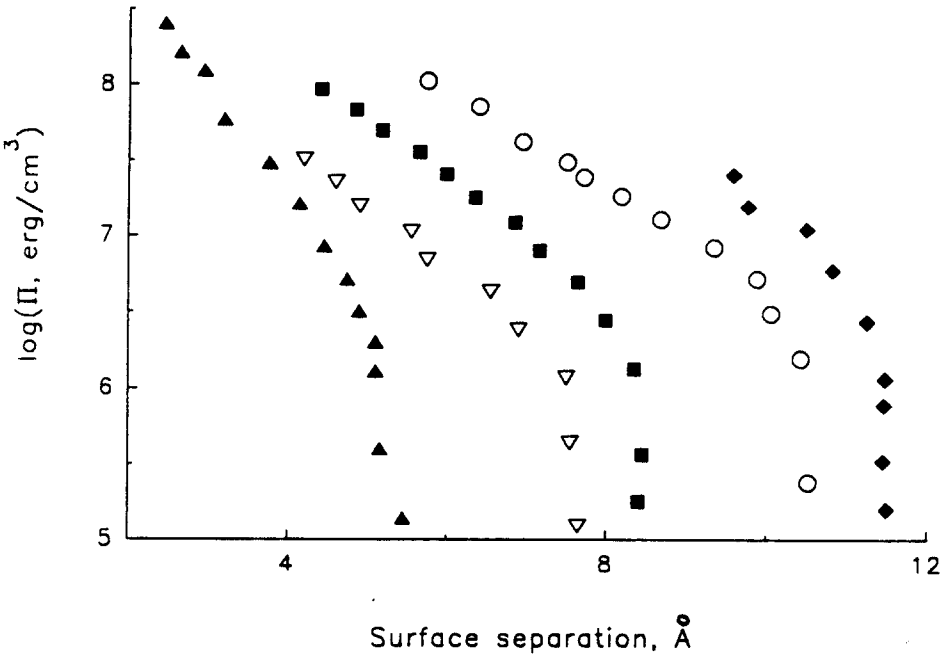

Figure 3 Osmotic pressure vs surface separation data are compared for several spontaneously assembled systems. (▲) Reconstituted rat tail tendon collagen in water at pH 7.5. (▽) DNA in 50 mM $MnCl_2$ at 50°C, (■) DNA in 20 mM $Co(NH_3)_6Cl_3$ and 0.25 M NaCl, (○) DNA precipitated by salmon protamine (a small, basic polypeptide used in packaging DNA in sperm heads); (◆) POPE in water. Table 1 summarizes exponential force parameters. The attractive force balancing the residual hydration repulsion for these materials appears significantly larger than expected for a van der Waals interaction.

As Figure 4 illustrates, osmotic stress can induce abrupt transitions between the limiting 3- to 4-Å and 1.3- to 1.5-Å decay length curves of DNA. These transitions, which are accompanied by sudden changes in spacing, occur at subcritical concentrations of DNA-condensing cations as $Co(NH_3)_6^{3+}$. The transition pressure decreases with increasing cation concentration (55, 56). Alternatively, the temperature sensitivity of the Mn^{2+}-DNA assembly is evident in the osmotic stress curves at subcritical temperatures. Transition pressures in this case decrease with increasing temperature.

The temperature sensitivity of hydration forces between Mn^{2+}-DNA (Figure 4) (56) or collagen molecules (13) can be used to measure the entropic part of the interaction free energy. Because a force is a distance derivative of a work/free energy and the temperature derivative of a free energy is an entropy, one can reconstruct the entropy and the enthalpy vs molecular separation from the force measurement. The result for Mn^{2+}-DNA is an entropy that itself *increases exponentially* as molecules are brought together (67).

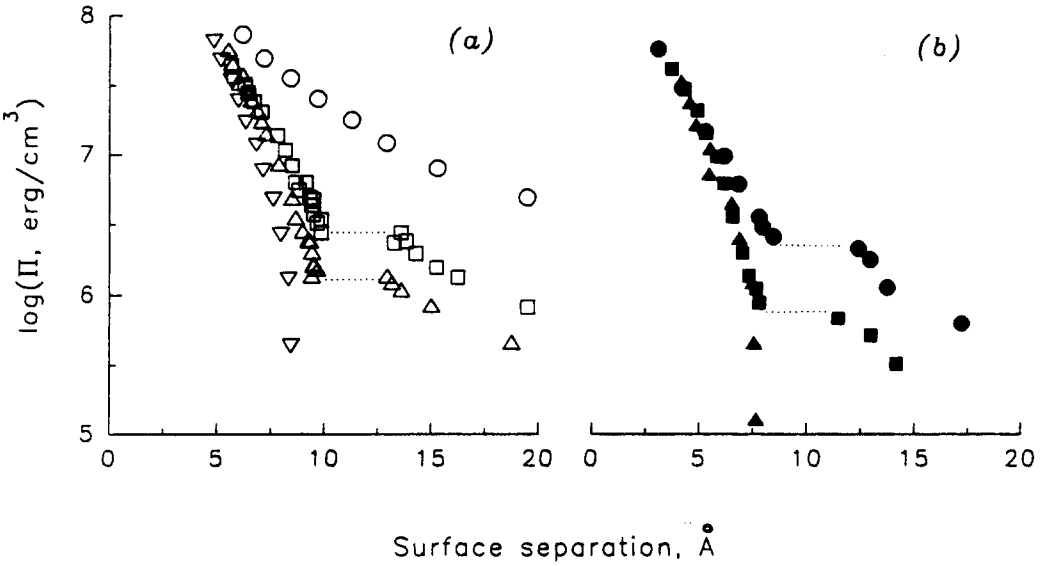

Figure 4 Typical osmotic stress-induced transitions in DNA-packing and hydration-force curves observed in the presence of DNA-condensing counterions. The transition from the 3- to 4-Å decay length (characteristic for most mono- and divalent counterions) to the ~1.5-Å decay length (associated with residual repulsion between spontaneously assembled helices) is accompanied by an abrupt change in separation. (*a*) The osmotic stress curves for Co^{3+}-DNA in 0.25 M NaCl are shown with varying $Co(NH_3)_6Cl_3$ concentrations: (○) 0 mM, (□) 8 mM, (△) 12 mM, and (▽) 20 mM. Spontaneous assembly with no applied osmotic stress requires ~17 mM cobalt hexammine at this NaCl concentration. (*b*) The osmotic stress curves for Mn^{2+}-DNA in 50 mM $MnCl^{2+}$ are shown at 5°C (○), 35°C (■), and 50°C (▲). Precipitation occurs spontaneously at about 40°C for this Mn^{2+} concentration.

Glasses, Clays, and Minerals

X-ray studies of clay swelling (16, 68), analyses of capillary phenomena and water adsorption on solid surfaces (for a review see 69), and force-balance measurements between minerals (20, 32, 54, 70–73) and glasses (21, 22, 26, 54, 74) have also indicated upward breaks from the expected electrostatic double-layer repulsion at small distances.

The additional force measured between silica (glass) surfaces appears to be smooth, salt-independent, and exponential, with characteristic decay of about 5–10 Å (after subtracting the extrapolated double layer and the expected van der Waals interactions) (21, 22, 26, 54, 74).

Oscillatory forces have been reported between molecularly smooth mica surfaces (72, 75), in agreement with multiple spacings observed in clays exposed to controlled water vapors (17). The periods of oscillation seem to be different even for NaCl and KCl solutions (72, 75). After averaging the oscillations, an additional repulsion remains that apparently depends on the kind and concentration of salt adsorbed on mica (70–73). One report has also indicated that the force curves for mica in ionic solutions cannot be reproduced after modifying the water purification procedure (33).

The deviations from double-layer force encourage one to think that glasses and minerals also experience hydration repulsion. Still, these deviations should be regarded with circumspection, given ambiguities posed by (*a*) subtraction of theoretically expected or extrapolated double-layer and van der Waals forces, (*b*) surface roughness of glasses, (*c*) glass/mica/glue deformation at high pressure (28–31; P. Kekicheff, S. Marcelja, T. J. Senden & V. E. Shubin, submitted), (*d*) surface contamination (33, 34), and (*e*) degradation of mica mounting attacked by salt (32; P. Kekicheff, S. Marcelja, T. J. Senden & V. E. Shubin, submitted).

Some Lessons and an Overview

A similar short-range, ionic strength–independent, exponentially varying repulsion seen between charged, net neutral ionic, and totally uncharged polar surfaces of very different chemistry suggests a common, underlying origin. The identical force curves measured for DNA and lipid (DDP) bilayers in TMA^+ identify the source of the interaction as surface polar groups, the only structural feature shared by these two materials. The same planar decay length (see Table 1) seen for DNA, polysaccharides, DDP bilayers, and glasses further suggests that there exists a natural decay length for the force in water. Oscillatory forces observed between stiff, molecularly smooth mica surfaces appear to be an immediate consequence of discrete layering of boundary solvent. These oscillations do not occur

in any other system discussed, in which the layering is apparently prevented by surface roughness or flexibility.

An argument sometimes raised against a common nature of the exponential short-range forces (9, 76) is that there are differences in the force decay length, λ, among the systems studied. In several cases, in particular for forces measured between solid surfaces using force-balance methods, the variability in λ can be attributed to ambiguities inherent in the subtraction of theoretically expected double-layer and van der Waals forces. Still, small λ values of $\sim$1–2 Å seen for collagen, DNA, and most lipid bilayers, as well as changes in λ produced by modifications in the surface structure of lipid bilayers or DNA, are now well documented and any theory must account for them.

We now discuss various attempts and their shortcomings to explain the experimental results within theories of electrostatic and entropic forces. Then we turn to the idea that hydration forces reflect the work of removing water organized around hydrophilic surfaces. The formalism that has been developed for this solvent structuring force, when applied to systems with discrete surface groups bearing unlike charges, can account for both the repulsive and the attractive hydration forces seen as well as provide the link connecting the observed decay length with not only solvent but also surface structure.

THEORETICAL DESCRIPTIONS OF HYDRATION FORCES

Electrostatic Double-Layer and Image-Charge Models

Exponential, salt-independent forces, whose decay lengths bear little resemblance to Debye lengths, cannot be explained by traditional electrostatic double-layer theory. When the double layers are formed mostly by counterions, the electrostatic interaction might become salt independent, but then at small separations it should decay roughly as the inverse square of separation (4). Even the earliest systematic measurements on zwitterionic lipids in distilled water (8, 65) already demonstrated that the counterion-only version of double-layer forces between lipid bilayers (77, 78) could not work.

Other kinds of electrostatic theories, particularly ones that recognize the "image-charge forces" acting on lipid polar group zwitterions near hydrocarbon/water boundaries, have also been elaborated (79–89). These models use definitions of separation different from those in the actual experiment and certainly never reproduce the sustained four-decades-wide exponential variation often seen with lipids (e.g. Figure 1). These models predict a weaker salt concentration dependence than does double-layer

theory (A. A. Kornyshev, D. A. Kossakowski & S. Leikin; in preparation), but they still cannot explain the absence of any salt dependence observed in experiment. Even the magnitude of predicted image forces is problematic. This interaction is strong enough to contribute to the hydration force only if one introduces a nonlocal dielectric response that effectively lowers the dielectric constant of water (87).

Concomitant to the image-charge repulsion between polar groups and the dielectric interface is the direct interaction of apposing discrete charges themselves. Laterally mobile zwitterions or adsorbed ions are driven to energetically favorable configurations so as to create a net attraction between the apposing surfaces. The strength of charge correlation depends on charge mobility, temperature, and surface defects. Variation in these factors can result in electrostatic charge-correlation attraction being stronger or weaker than image-charge repulsion (81–89).

Configurational/Entropic Forces

UNDULATORY FORCES Because of their inherent flexibility, membranes and linear macromolecules experience thermally driven shape fluctuations. Crowding of neighbors entails a reduction in configurational entropy and a consequent "steric" repulsion. Although molecular collision alone is expected to cause long-range repulsion between membranes (90) or between linear molecules (91–93), the force has the form of a power law rather than an exponential. [One exception to this is the exponentiality of a "blister" model with membranes bulging away from a supporting substrate (94, 95). This model is explicitly intended to apply to interactions between bilayers on mica and not to the multilayer assemblies in which the exponential variation of hydration forces has been quantitatively determined.]

The configurational/entropic power law has been demonstrated at large distances between weakly interacting, flexible layers in multilamellar systems (96, 97). In contrast, Figure 1 illustrates exponentiality of the short-range force between egg PC bilayers seen over 4 decades in pressure, or over 10 decay lengths. Forces measured between many other lipid bilayers (10, 38, 40, 50, 59) and between collagen molecules at pH 6 (S. Leikin, D. C. Rau & V. A. Parsegian, in preparation) also show exponentiality for at least 3–4 decades in pressure. Attempts to fit measured forces between DNA helices by the power law of purely steric or undulatory repulsion have not worked either (98).

Other evidence suggests the unlikelihood of an entropic-undulatory origin of hydration forces. In particular, identical forces are measured by OS and SFA between free and between immobilized bilayers from the same frozen-chain lipids (27, 35). Identical hydration forces have been observed through OS for melted and frozen forms of a synthetic charged

lipid (35) wherein strong repulsion appears to have suppressed all significant undulation.

Only at low pressures, when fluid bilayers or flexible molecules collide through the soft, exponential potentials of direct interactions, do undulatory forces appear appreciable in the systems in which force measurements have been made (27, 35, 45, 53, 99, 100). In this case, observed exponential variation of a net force, with decay lengths roughly two times larger than expected, can be explained by mutual enhancement of the undulatory and direct hydration (or electrostatic double-layer) forces (53, 98, 99, 101).

HEAD GROUP COLLISIONS Collisions on a smaller scale have also been considered; for example, those between thermally disordered polar head groups. However, an early upper-bound estimate of this interaction (78) predicted forces much smaller than those directly measured a few years later (8). Elaborate computer simulations of steric repulsions between colliding polar heads (102, 103) seem rather to fit an upward break in the hydration force curve seen at 3–5 Å (59, 104), if one shifts the bilayer separations used in the original theory to coincide with experimental definitions (T. J. McIntosh, private communication). Indeed, it has been argued that this upward break, which is not seen when polar groups are spread out by added cholesterol, is caused by molecular contacts between the opposing polar heads (59).

MOLECULAR PROTRUSIONS In a molecular protrusion model, individually emergent lipid molecules are expected to create a pressure on the apposing bilayer surface as far as 15–20 Å away (76, 105). For an upper bound estimate, proponents consider the work of emergence to be determined only by the surface tension γ of a newly created hydrocarbon/water interface and neglect the energy of the hole left by the emerging molecule. The opposing bilayer is modeled by a hard wall. The pressure then decays exponentially with characteristic length $\lambda = kT/\pi\delta\gamma$, where δ is the effective diameter of a lipid molecule (105). Using $\delta \approx 7$–8 Å for double-chain lipids and $\gamma \approx 50$ dyn/cm (9, 106), we find the expected upper bound for λ to be only approximately 0.3–0.4 Å, whereas observed λ ranges from 1–3 Å for neutral phospholipids to approximately 5 Å for DDP (Table 1). Only by using $\gamma \approx 18$ dyn/cm does one manage to extract a more reasonable $\lambda \approx 2$ Å (106), but only for $\delta \approx 4$ Å, which corresponds to a single-lipid chain.

It has been argued that this force does not contribute to the hydration repulsion (107). Protrusion of the required amount would produce unreasonably high molecular solubilities (108). Even a correlation with molecular solubility, inherent in the protrusion model, is not seen experimentally, where hydration forces between much more soluble single-chain

lysoPC in the lamellar phase are similar to those between double-chain egg PC (109). In addition, protrusion from rigid, well-defined DNA or silica surfaces is not even possible. Yet, the identical hydration force has been measured between DDP bilayers and between DNA molecules. These are just several examples of numerous observations (62, 107) that demonstrate the unlikelihood of the protrusion model. However, molecular protrusions can still contribute to the upward breaks from lipid hydration force curves at distances less than 3–5 Å.

Solvation Models

A common feature of all the systems we present here is that surface polar and charged groups strongly bind and restructure water. Soon after the first report of exponentially varying forces between neutral bilayers in distilled water, Marcelja & Radic (110) suggested that the forces could result from solvent perturbation by the membrane surface. To allow all kinds of perturbation, they adapted the Landau-Ginsburg order-parameter formalism (111) originally developed to describe second-order phase transitions. The simple but elegant language of that formalism, despite its frustrating agnosticism as to the character of incurred perturbation, has been articulated to allow one to speak of hydration forces in all materials where they have been encountered. In particular, generalizations of the Marcelja-Radic model have given a rationale for observed variation of force parameters between these materials (38, 112–114). Before more detailed discussion of these models in the next section of this review, we consider interpretations suggested for the physical nature of the order parameter, not specified in the original formulation.

NONLOCAL ELECTROSTATICS Electric polarization was first suggested as the pertinent water order parameter (115, 116). This idea was generalized later within nonlocal electrostatic theory, which accounts for nonlocal response of the polarization to a remote electric field (117–122).

A major difficulty with nonlocal electrostatic response phenomenology is choosing the correct form of the nonlocal dielectric susceptibility function in water. Several applications of the nonlocal electrostatic theory (123) have successfully used an exponential form, but recent arguments have maintained that the response in bulk water might be nonexponential (124–128). This problem remains unresolved (129). In addition, in a narrow gap between two surfaces an effective, average dielectric response might be modified by surface roughness and thermal motions typical of most systems studied. In particular, recent computer simulations show that small thermal motions of lipids wipe out characteristic oscillating profiles, resulting in a smooth, exponentially varying polarization between two apposing

lipid bilayers (130; S. J. Marrink, M. Berkowitz & H. J. C. Berendsen, in preparation).

A nonlocal dielectric response theory also predicts a coupling between the water correlation length, λ_w, and the Debye shielding length, λ_D. This coupling causes a change in the apparent values of both λ_w and λ_D; specifically, it should create a salt-concentration dependence of λ_w and conversely modify λ_D (115, 119, 131–133). However, neither one of these effects has been observed in hydration (53) or double-layer (9, 47, 48, 50, 53, 70, 74) force measurements.

HYDROGEN BONDING Nonlocal dielectric response is, to a large but uncertain extent, a result of hydrogen bonding between water molecules. In a nonelectrostatic approach, the order parameter can be directly associated with reorganization of the hydrogen-bond network in water.

Hydrogen bonding involves very large energies, ≈ 5 kcal/mol, about the same as the hydration energy of a PC polar head. A hydrogen-bonded network that is transient but extensive provides a mechanism for extending the reorganization of water in contact with a polar surface out into the solution. This mechanism is supported by several computer simulations (130, 134–136) and by experimental evidence (137), indicating that the ability of lipids to swell in different solvents is correlated with the hydrogen-bonding capability of the liquid.

More detailed molecular models based on hydrogen bonding are in a very early stage of development (138, 139). Progress is encouraging but still hobbled by the difficulties intrinsic to the theory of associated liquids.

SOLVATION THEORY: CONNECTING MOLECULAR STRUCTURE WITH INTERACTIONS

Order Parameter Model

In this model, reorganization of solvent around polar groups is represented by an order parameter η with a fixed value at the apposing polar surfaces and a zero value in the bulk solution (110). To leading terms, the difference in the free energy density from that of pure solvent goes as the square of η and of the gradient of η (111). The work required to bring two surfaces together is automatically a work to transfer perturbed water from between the surfaces to the outside solution.

From this perspective, it is remarkable that very weak perturbations of water translate into large forces. Even the highest levels of osmotic stress, $-\Pi_{osm} \approx 10^9$ erg/cm^3, correspond to chemical potential differences, $\Delta\mu_w = \Pi_{osm} v_w$, on the order of thermal energy, $kT \approx 4 \times 10^{-14}$ erg or $RT \approx 0.6$ kcal/mol, (v_w is the 18 cm^3 molar or 30 Å^3 molecular volume of water). For further discussion on this point see Parsegian et al (14).

This order-parameter formalism, mathematically equivalent to the Debye-Huckel theory applied to the electrostatic double layer interactions, predicts a repulsive hydration pressure P_{rep}^{hom} between two similar, homogeneous planar surfaces separated by the distance L (110),

$$P_{rep}^{hom} = \frac{C_{rep}}{\sinh^2(L/2\lambda_w)}, \qquad 2.$$

and an attractive pressure (140),

$$P_{attr}^{hom} = -\frac{C_{attr}}{\cosh^2(L/2\lambda_w)}, \qquad 3.$$

between two complementary surfaces. The force coefficients C_{rep} and C_{attr} incorporate the magnitude of the solvent order parameter at each surface (110, 140).

This formalism gives a straightforward connection between perturbation of the solvent structure and measured exponential forces. When separation L is much greater than the decay length λ_w, both P_{rep}^{hom} and P_{attr}^{hom} go over to exponentials, $4C_{rep}\exp(-L/\lambda_w)$ and $4C_{attr}\exp(-L/\lambda_w)$, decaying with a solvent-characteristic length λ_w (formally analogous to Debye length). Force amplitudes depend on the extent of the surface perturbation and on the strength of solvent-solvent interaction.

Mean Field Model

In further development of these ideas, measured forces have been related to structural features of the interacting surfaces (112–114). One can use the order-parameter language and speak of mean solvation force fields produced by discrete polar groups. Charged, dipolar, or hydrogen-bond forming polar groups can be formally represented by "hydration charges" (Figure 5). Hydration force parameters can then be connected to the surface distribution of these "charges" (112, 113).

LATERALLY INHOMOGENEOUS, NET NEUTRAL PLANAR SURFACES Figure 5 illustrates a model for interaction between two plane-parallel surfaces with discrete point "hydration charges" but no net charge, $P_{rep(attr)}^{hom} = 0$. Because of this model's similarity to Debye-Huckel theory, one can speak of an inhomogeneous density of "hydration charges" $\rho(x,y,z)$. We will treat separately the case of polar groups distributed parallel $\rho(x,y)$ and perpendicular $\rho(z)$ to the surface.

Writing a surface "hydration-charge" density $\sigma(x,y) = \sigma(\mathbf{R})$, where $\mathbf{R}$ is a vector in the (x,y) plane, one can speak of surface periodicities. Specifically, in analogy to X-ray or neutron diffraction, the surface can be described by the structure factor

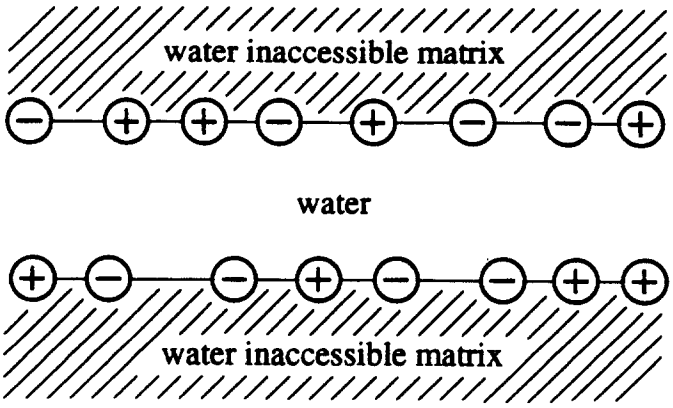

Figure 5 Interacting net neutral polar surfaces modeled as a set of equivalent "hydration charges" on the interface between water and a hydrophobic substrate. The "hydration charge" produces a solvation force field, a combination of electric polarization and a perturbation in the water hydrogen-bond network. The total interaction involves not only that between facing "charge" configurations but also repulsion between each set of "hydration charges" and the apposing wall. Two such plane-parallel surfaces will repel or attract depending on the extent of mutual complementarity in their polar group distributions.

$$S(\mathbf{Q}) = \int d\mathbf{R} \langle \sigma(\mathbf{r}+\mathbf{R})\sigma(\mathbf{r}) \rangle e^{-i\mathbf{QR}}, \qquad 4.$$

which gives an average contribution from every wave vector $\mathbf{Q}$ (or surface periodicity) to $\sigma(\mathbf{R})$ (112) (<..> designates an ensemble average or an **r**-average over the interacting surfaces).

The repulsive part of the force between two identical surfaces with no net "hydration charge" (112, 113)

$$P_{\text{rep}}^{\text{inhom}} = \frac{\alpha}{4\pi^2} \int d\mathbf{Q} \frac{S(\mathbf{Q})}{\sinh^2 [L(\lambda_w^{-2} + Q^2)^{1/2}]}$$

is a sum of contributions from all surface periodicities. The parameter α gives the strength of water reorganization by the surface groups. (For illustration one can again use the analogy with the Debye-Huckel theory where λ_w would be a Debye length and $\alpha = 4\pi\varepsilon_w^{-1}$.)

For ordered surfaces with periodicity a, the force

$$P_{\text{rep}}^{\text{inhom}} = \frac{\alpha \langle \sigma^2 \rangle}{\sinh^2 \{L[\lambda_w^{-2} + (2\pi/a)^2]^{1/2}\}}, \qquad 6.$$

is proportional to the mean-square value $<\sigma^2>$ of the surface "hydration-charge" density. The new decay length,

$$\lambda = \frac{1}{2[\lambda_w^{-2} + (2\pi/a)^2]^{1/2}}, \qquad 7.$$

now reflects both the surface and the solvent structure (112).

For surfaces with negligible short-range order the force is dominated by contributions from smaller **Q** and the decay length is half the water correlation length ($\lambda = \lambda_w/2$) (112). With increasing surface order we expect the decay length as well as the absolute value of the force at large distances to decrease while the preexponential factor should increase (112, 113).

CHARGED PLANAR SURFACES One can think of the repulsive hydration force between two planar polar surfaces as the sum (112)

$$P_{rep} = P_{rep}^{hom} + P_{rep}^{inhom}. \qquad 8.$$

The homogeneous repulsion P_{rep}^{hom}, given by Equation 2, comes from a nonzero average "hydration-charge" density. The inhomogeneous component of the force, P_{rep}^{inhom}, is produced by balanced discrete "hydration charges," which do not contribute to the average density and dominate the interaction in systems with no net charge.

INTERFACIAL THICKNESS AND ROUGHNESS Inhomogeneities $\rho(x,y,z)$ in the direction (z) normal to the surfaces represent finite thickness and roughness of real interfaces, which might have an impact on the force. A first step toward incorporation of these features into models of hydration forces has been made within the nonlocal electrostatic approach (114) for a surface "polarity profile" $\rho(z)$ varying only in the normal direction. It has been argued that the effect of such $\rho(z)$ for lipid/water interfaces might increase the observed decay length (114).

Reexamination of Measured Hydration Forces

The fact that the same decay length of 4–5 Å is seen for highly charged didodecylphosphate (DDP) bilayers and DNA molecules with TMA^+ counterions, for charged and uncharged polysaccharides, and for glasses (see Table 1) suggests that this length is the water correlation length λ_w. The same estimate for λ_w has been obtained from totally independent experiments (123, 141, 142). In contrast to zwitterionic phospholipids or net neutral ionic surfaces, these materials would reasonably be expected to have a net surface "hydration charge" and show forces dominated by the homogeneous repulsion, P_{rep}^{hom}. Using this as a working hypothesis, we can now reexamine the variation of hydration force parameters seen in different systems.

Table 1 compares theoretically predicted decay lengths with the measured values. The residual repulsion of spontaneously assembled DNA

and collagen are expected to reflect the inhomogeneous force for net neutral surfaces, P_{rep}^{inhom}. Taking an average 34-Å helical pitch for net neutral Mn-DNA or Co-DNA as the surface periodicity a and using Equation 7, we find the decay length, λ, of 1.6–1.8 Å in good agreement with the measured value of about 1.3 Å. Because of surface curvature, the effective λ for cylindrical molecules at close spacing should be slightly smaller than predicted by Equation 7 for planar surfaces. The decay length similarly calculated for collagen with a 9.6-Å helical repeat is 0.7 Å, compared with the observed 0.6 Å.

The decay lengths for net neutral lipid bilayers are also expected to reflect the inhomogeneous force and to depend on surface ordering (112). Equation 7 predicts a limiting value of 0.7 Å for strongly ordered polar heads with $a \approx 8$ Å, which was estimated from the surface area per head group. The decay length is expected to increase with surface disordering up to a limiting value of 2.0–2.5 Å ($\lambda_w/2$). For charged lipid bilayers both P_{rep}^{hom} and P_{rep}^{inhom} can contribute to the total force, where P_{rep}^{hom} decrease and P_{rep}^{inhom} increase with adsorption of counterions. The effective value of λ ranges anywhere from 0.7 to 5 Å, depending on counterion adsorption, surface separation, and surface structure.

We can now relate the difference in the force to the structure of lipid bilayers. In particular, the most important difference between net neutral PE and PC bilayers is in the ability of PE polar heads to form lateral hydrogen bonds with each other. The stronger lateral order of PE bilayers, indicated also by smaller areas per headgroup (38), explains the shorter λ and larger P_o observed for PE. Single PE methylation, because it destroys the capacity for lateral hydrogen bonding, results in force parameters similar to those for PC. Two component PE/PC bilayers might repel more strongly than one would predict from a linear superposition owing to the disordering effect of lipid mixing.

Other examples of the disordering effect of lipid mixing can explain the physical nature of the puzzling strengthening of hydration forces between PC bilayers that occurs with removal of PC polar heads. Added diacylglycerol (PC without the polar head), acting as a hydrophobic spacer, is expected to result in increasing λ and stronger hydration and decreasing surface polarity and P_o. This has been observed (64; J. Bech & R. P. Rand, in preparation).

Predictably, packing of lipid chains appears to have a strong impact on polar head ordering. Adding to the list of examples, chain heterogeneity and melting might explain the observed (10, 15, 38, 40) increase in the decay length and in lipid hydration. Phosphorylcholine molecules (PC polar heads) on their own precipitate from solution and crystallize at concentrations far lower than in PC multilayers (143). Their attachment

to the bilayer surface apparently frustrates the attraction they would otherwise express.

A change in polar head ordering resulting from added cholesterol might be responsible for complex changes observed (10, 40, 59, 62) in the force parameters, including significant variation in the decay length.

Hydration Attraction and Molecular Recognition

In addition to hydration repulsion, interaction between net neutral surfaces involves attraction between facing groups with unlike "hydration charges" mediated by the same force fields. Two surfaces attract to the extent of the mutual complementarity in their polar-group distributions. This assumption, originally inferred from experimental observations (140), fits well within the logic of the order-parameter theory (38, 113, 140, 144).

HYDRATION ATTRACTION Attractive hydration force between two complementary "featureless" surfaces is given in Equation 3. The theory of attractive hydration forces between surfaces with discrete polar groups, which requires complicated formulation of intersurface correlations, is still in a very early stage of development (113).

For two similar net neutral surfaces with mobile polar groups, like those of fluid phospholipid bilayers, this force is analogous to the ion-correlation attraction discussed earlier. At low temperatures, hydration attraction should become stronger than hydration repulsion and induce formation of dehydrated contact between surfaces (88, 113). At present, the temperature of this dehydration transition cannot be accurately predicted (88, 113). Very small equilibrium spacings ($\leqslant 5$ Å) or even completely dehydrated contacts have been observed between some PEs (15, 38, 145, 146) and between acidic phospholipids neutralized by divalent cations (147–149). Surface disordering, inhomogeneity, and defects reduce this correlation attraction and, correspondingly, strengthen repulsion (88, 113). This predicted breakage of correlated attractive surfaces might, for example, explain an otherwise puzzling observation (150) in which spontaneously dehydrated pure phosphatidylserine bilayers neutralized by Ca^{2+} swell upon addition of 40 mol% largely hydrophobic diacylglycerol molecules.

In a similar way, a correlation between fixed phosphate groups and mobile, bound tri- and multivalent cations can explain the spontaneous assembly of DNA and the apparent magnitude of the attractive force (55).

MOLECULAR RECOGNITION Two surfaces with structure factors $S_1(\mathbf{Q})$ and $S_2(\mathbf{Q})$ are expected to attract according to an integral over all possible surface structure periodicities (S. Leikin & V. A. Parsegian, submitted),

$$P_a' \cong -\frac{\alpha^2}{\pi^2}\int d\mathbf{Q}\frac{S_1(\mathbf{Q})S_2(\mathbf{Q})}{kT(\lambda_w^{-2}+Q^2)^{1/2}}\exp[-2L(\lambda_w^{-2}+Q^2)^{1/2}]. \quad 9.$$

One sees clearly the increase in attraction with stronger overlapping structure factors $S_1(\mathbf{Q})$ and $S_2(\mathbf{Q})$. Specifically, the product $S_1(\mathbf{Q})S_2(\mathbf{Q})$ becomes a measure of complementarity between the apposing surfaces. When two surfaces match poorly, the product is small at any particular value of $\mathbf{Q}$; attraction is weak, and we expect the net force to be repulsive. This is, heuristically, an intuitive mechanism for molecular recognition via hydration forces (S. Leikin & V. A. Parsegian, submitted).

Two imperfectly matching surfaces can still recognize each other, but only to the extent of the $S_1(\mathbf{Q})$, $S_2(\mathbf{Q})$ similarity evaluated by the integral of $S_1(\mathbf{Q})S_2(\mathbf{Q})$. Remarkably, in this case of imperfect matching, elevated temperature might actually facilitate recognition by easing the "hydration charges" out of fixed positions and allowing the apposing surfaces to adopt better-matching, complementary "charge" distributions. We expect the mutual approach of the surfaces to be followed by exponentially increasing conformational entropy of the polar groups, unless the separation becomes too small to allow any motion (S. Leikin & V. A. Parsegian, submitted).

A rapid increase in hydration attraction upon heating has been seen in Mn-DNA aggregates (56) as well as between collagen molecules (13). For the Mn-DNA system one actually measures an exponential increase in entropy vs separation as DNA molecules are brought together (67). Whether this entropy and temperature strengthening of attraction result from molecular rearrangement or from release of surface-structured water into bulk solution (56, 67) is difficult to tell. Both possibilities fit well within the molecular events associated with hydration forces.

HYDRATION-MOTIVATED PHENOMENA

Forces as powerful and specific as those described here can be expected to have many kinds of organizing consequences. One should be aware of their potential for action in many kinds of systems.

A delicate balance between repulsive and longer-range attractive hydration forces can underlie recognition and assembly of polar macromolecules. At molecular contact—in protein-DNA interactions, in membrane fusion, in antigen-antibody or ligand-receptor binding—the strongest part of the operative energy probably comes from the hydration forces that dominate force/distance curves. Here one might expect packing transitions, like those seen for DNA at subcritical concentrations of condensing counterions (55, 56).

From what we already know about the strength and specificity of

hydration forces emerges a new language of contact and transformation, a language that combines the words of molecular structure through a grammar of solvent perturbation. Indeed, the very idea of a solvation force, with its constituent entropies and enthalpies of water release, prepares us to refine and to elevate traditional solvation concepts such as "hydrophobic bonding" to include the new and infinitely greater molecular-design possibilities of polar surfaces. Hydration forces between such surfaces will be far more specific than those between nonpolar surfaces; their strength will be such as to induce structural changes in mutually approaching polar surfaces or the docking of a ligand effector to a large molecule. There can be a natural link between the nanomechanics of an allosteric protein and the powerful fit-inducing tug of enforced complementarity in contact.

The same osmotic stress technique that measures forces between molecules or membranes has now shown its power to measure forces within them. For example:

1. Experimental evidence suggests that phase transitions such as B-A and B-Z transitions in DNA double helices (151), chain freezing in lipid bilayers (152, 153), or transitions between lamellar and nonlamellar forms of phospholipids (154) are related, at least in part, to the action of hydration force fields. For lipids in lamellar phases, several phenomenological models of the coupling have been proposed (144, 152, 153, 155–157).
2. A transmembrane ionic channel will shut under the osmotic stress of solutes too big to enter the aqueous space meant only for small molecules; osmotic sensitivity can tell us the change in the number of solute-inaccessible water molecules as the channel moves from open to closed form (158–161). One might expect a functionally significant energetics of aqueous cavity formation within channels, much as there is an energetics of hydration interaction between molecules.
3. Large proteins in solution—hemoglobin (162), cytochrome oxidase (163), hexokinase (164)—move between different conformations corresponding to different functioning states, with an osmotic sensitivity that suggests different degrees of solvation in the different forms. Does the solvent exposure of protein surfaces that go with these allosteric transitions entail the same large energies that one measures when protein surfaces are brought together against hydration forces? Solvation energies are significant on the scale of bioenergetics where the energy of ATP hydrolysis is about the same as the hydration energies we measure.

We have more questions than answers. Only the first tentative steps have been taken toward understanding these phenomena. Newly measured

forces of course demand further theoretical analysis, but the lack of that analysis should not impede practical use.

The forces that have been measured are neither predicted by nor introduced into any computer program for protein folding, interaction, molecular design, or any other application. After all, the absence of any good theory for dielectric constants has not prevented the use of phenomenological theories based on empirical rules. Electrostatic calculations even go beyond these simple theories, using multiparameter models of water and artificial, spatially varying dielectric constants. There is no reason why this important part of almost any computer algorithm cannot be based on directly measured forces.

At the very least, the consequence of water activity on molecular interaction and structure as well as on function and regulation is every bit as interesting as the activity of protons, ions, solutes, and ligands. The power to think of water as an active system component has brought us to hydration forces. Why not look further at its action on the functioning molecule itself?

ACKNOWLEDGMENTS

This work was partly supported by an Office of Naval Research grant (N00014-91-F-0201) to V.A.P. and a National Science and Engineering Research Council of Canada grant to R.P.R.

Literature Cited

1. Derjaguin, B. V., Landau, L. 1941. *Acta Physicochim. URSS* 14: 633–62
2. Verwey, E. J. W., Overbeek, J. Th. G. 1948. *Theory of the Stability of Lyophobic Colloids*. Amsterdam: Elsevier
3. Parsegian, V. A. 1973. *Annu. Rev. Biophys. Bioeng.* 2: 221–55
4. Langmuir, I. 1938. *J. Chem. Phys.* 6: 873–96
5. Derjaguin, B. V., Kusakov, M. M. 1939. *Acta Physicochim. URSS* 10: 153
6. Derjaguin, B. V., Churaev, N. V. 1974. *J. Colloid Interface Sci.* 49: 249–55
7. Ninham, B. W. 1985. *Chem. Scr.* 25: 3–6
8. LeNeveu, D. M., Rand, R. P., Parsegian, V. A. 1976. *Nature* 259: 601–3
9. Israelachvili, J. N. 1991. *Intermolecular and Surface Forces*. London: Academic. 450 pp. 2nd ed.
10. Rand, R. P., Parsegian, V. A. 1989. *Biochim. Biophys. Acta* 988: 351–76
11. Rau, D. C., Lee, B. K., Parsegian, V. A. 1984. *Proc. Natl. Acad. Sci. USA* 81: 2621–25
12. Rau, D. C., Parsegian, V. A. 1990. *Science* 249: 1278–81
13. Leikin, S., Rau, D. C., Parsegian, V. A. 1993. *Biophys. J.* 64: A270
14. Parsegian, V. A., Rand, R. P., Fuller, N. L., Rau, D. C. 1986. *Methods Enzymol.* 127: 400–16
15. McIntosh, T. J., Simon, S. A. 1986. *Biochemistry* 25: 4058–4066
16. Viani, B. E., Low, P. F., Roth, C. B. 1983. *J. Colloid Interface Sci.* 96: 229–44
17. Bradley, W. F., Grim, R. E., Clark, G. L. 1937. *Z. Kristallogr. Kristallgeom. Kristallphys. Kristallchem.* 97: 216
18. Jendrasiak, G. L., Hasty, J. H. 1974. *Biochim. Biophys. Acta* 337: 79–91
19. Jendrasiak, G. L., Mendible, J. C. 1976. *Biochim. Biophys. Acta* 424: 149–58
20. Israelachvili, J. N., Adams, G. E. 1978. *J. Chem. Soc. Faraday Trans.* 1 74: 975–1001
21. Rabinovich, Ya. I., Derjaguin, B. V., Churaev, N. V. 1982. *Adv. Colloid Interface Sci.* 16: 63–78

22. Peschel, G., Belouschek, P., Muller, M. M., Muller, M. R., Konig, R. 1982. *Colloid Polym. Sci.* 260: 444–51
23. Lubetkin, S. D., Middleton, S. R., Ottewill, F. R. S. 1984. *Philos. Trans. R. Soc. London Ser. A* 311: 353–68
24. Parker, J. L. 1992. *Langmuir* 8: 551–56
25. Butt, H.-J. 1991. *Biophys. J.* 60: 1438–44
26. Ducker, W. A., Senden, T. J., Pashley, R. M. 1992. *Langmuir* 8: 1831–36
27. Horn, R. G., Israelachvili, J. N., Marra, J., Parsegian, V. A., Rand, R. P. 1988. *Biophys. J.* 54: 1185–86
28. Parsegian, V. A., Rand, R. P., Fuller, N. L. 1991. *J. Phys. Chem.* 95: 4777–82
29. Horn, R. G., Israelachvili, J. N., Pribac, F. 1987. *J. Colloid Interface Sci.* 115: 480–92
30. Attard, P., Parker, J. L. 1992. *Phys. Rev. A* 46: 7959–71
31. Parker, J. L., Attard, P. 1992. *J. Phys. Chem.* 96: 10398–10405
32. Pashley, R. M., Israelachvili, J. 1984. *J. Colloid Interface Sci.* 97: 446–55
33. Dunsten, D. E. 1992. *Langmuir* 8: 740–43
34. Parsegian, V. A., Gershfeld, N. L. 1993. *Biophys. J.* 64: A222
35. Tsao, Y.-H., Evans, D. F., Rand, R. P., Parsegian, V. A. 1993. *Langmuir.* 9: 233–41
36. Tsao, Y.-H., Yang, S. X., Evans, D. F. 1992. *Langmuir* 8: 1188–94
37. Luzatti, V., Husson, F. 1962. *J. Cell Biol.* 12: 207–19
38. Rand, R. P., Fuller, N., Parsegian, V. A., Rau, D. C. 1988. *Biochemistry* 27: 7711–22
39. Evans, E., Needham, D. 1987. *J. Phys. Chem.* 91: 4219–28
40. Lis, L. J., McAlister, M., Fuller, N., Rand, R. P., Parsegian, V. A. 1982. *Biophys. J.* 37: 657–65
41. Horn, R. G. 1984. *Biochim. Biophys. Acta* 778: 224–28
42. Marra, J., Israelachvili, J. N. 1985. *Biochemistry* 24: 4608–18
43. Lis, L. J., Lis, W. T., Parsegian, V. A., Rand, R. P. 1981. *Biochemistry* 20: 1771–77
44. Afzal, S., Tesler, W. J., Blessing, S. K., Collins, J. M., Lis, L. J. 1984. *J. Colloid Interface Sci.* 97: 303–7
45. McIntosh, T. J., Magid, A. D., Simon, S. A. 1989. *Biophys. J.* 55: 897–904
46. Cowley, A. C., Fuller, N., Rand, R. P., Parsegian, V. A. 1978. *Biochemistry* 17: 3163–68
47. Loosley-Millman, M. E., Rand, R. P., Parsegian, V. A. 1982. *Biophys. J.* 40: 221–32
48. Marra, J. 1986. *Biophys. J.* 50: 815–25
49. Pashley, R. M., McGuiggan, P. M., Ninham, B. W., Brady, J., Evans, D. F. 1986. *J. Phys. Chem.* 90: 1637–42
50. McIntosh, T. J., Magid, A. D., Simon, S. A. 1990. *Biophys. J.* 57: 1187–97
51. Persson, P. K. T., Bergenstahl, B. A. 1985. *Biophys. J.* 47: 743–46
52. McIntosh, T. J., Magid, A. D., Simon, S. A. 1989. *Biochemistry* 28: 7904–12
53. Podgornik, R., Rau, D. C., Parsegian, V. A. 1989. *Macromolecules* 22: 1780–86
54. Grabbe, A., Horn, R. G. 1993. In *Proceedings of NATO Advanced Research Workshop on Clay Swelling and Expansive Soils*, ed. P. Bavete, M. B. McBride. Amsterdam: Kluwer Scientific. In press
55. Rau, D. C., Parsegian, V. A. 1992. *Biophys. J.* 61: 246–59
56. Rau, D. C., Parsegian, V. A. 1992. *Biophys. J.* 61: 260–71
57. Simon, S. A., McIntosh, T. J., Magid, A. D. 1988. *J. Colloid Interface Sci.* 126: 74–83
58. Simon, S. A., McIntosh, T. J. 1989. *Proc. Natl. Acad. Sci. USA* 86: 9263–67
59. McIntosh, T. J., Magid, A. D., Simon, S. A. 1989. *Biochemistry* 28: 17–25
60. Simon, S. A., Fink, C. A., Kenworthy, A. K., McIntosh, T. J. 1991. *Biophys. J.* 59: 538–46
61. Simon, S. A., McIntosh, T. J., Magid, A. D., Needham, D. 1992. *Biophys. J.* 61: 786–99
62. McIntosh, T. J., Simon, S. A., Needham, D., Huang, C. H. 1992. *Biochemistry* 31: 2020–24
63. Gawrisch, K., Ruston, D., Zimmerberg, J., Parsegian, V. A., Rand, R. P., Fuller, N. 1992. *Biophys. J.* 61: 1213–23
64. Das, S., Rand, R. P. 1986. *Biochemistry* 25: 2882–89
65. LeNeveu, D. M., Rand, R. P., Parsegian, V. A., Gingell, D. 1977. *Biophys. J.* 18: 209–30
66. Parsegian, V. A., Rand, R. P., Rau, D. C. 1987. In *Physics of Complex and Supermolecular Fluids*, ed. S. A. Safran, N. A. Clark, pp. 115–35. New York: Wiley
67. Leikin, S., Rau, D. C., Parsegian, V. A. 1991. *Phys. Rev. A* 44: 5272–78
68. Low, P. F. 1987. *Langmuir* 3: 18–25
69. Derjaguin, B. V., Churaev, N. V., Muller, V. M. 1987. *Surface Forces.* New York: Consultants Bureau
70. Pashley, R. M. 1981. *J. Colloid Interface Sci.* 83: 531–46
71. Pashley, R. M., Quirk, J. P. 1984. *Colloids Surf.* 9: 1–17

72. Pashley, R. M., Israelachvili, J. N. 1984. *J. Colloid Interface Sci.* 101: 511–23
73. Kjellander, R., Marcelja, S., Pashley, R. M., Quirk, J. P. 1990. *J. Chem. Phys.* 92: 4399–407
74. Horn, R. G., Smith, D. T., Haller, W. 1989. *Chem. Phys. Lett.* 162: 404–8
75. McGuiggan, P. M., Pashley, R. M. 1988. *J. Phys. Chem.* 92: 1235–39
76. Israelachvili, J. N., Wennerstrom, H. 1992. *J. Phys. Chem.* 96: 520–31
77. Parsegian, V. A. 1966. *Trans. Faraday Soc.* 62: 848–60
78. Parsegian, V. A. 1967. *Science* 156: 939–42
79. Jonsson, B., Wennerstrom, H. 1983. *Chem. Scr.* 22: 221–25
80. Jonsson, B., Wennerstrom, H. 1983. *J. Chem. Soc. Faraday Trans.* 2 79: 19–35
81. Kjellander, R. 1984. *J. Chem. Soc. Faraday Trans* 2 80: 1323–48
82. Attard, P., Mitchell, D. J. 1987. *Chem. Phys. Lett.* 133: 347–52
83. Attard, P., Mitchell, D. J. 1988. *J. Chem. Phys.* 88: 4391–96
84. Attard, P., Kjellander, R., Mitchell, D. J., Jonsson, B. 1988. *J. Chem. Phys.* 89: 1664–80
85. Jonsson, B., Attard, P., Mitchell, D. J. 1988. *J. Phys. Chem.* 92: 5001–5
86. Granfeld, M., Jonsson, B., Wennerstrom, H. 1988. *Mol. Phys.* 64: 129–42
87. Leikin, S., Kornyshev, A. A. 1990. *J. Chem. Phys.* 92: 6890–98; Erratum. 1991. *J. Chem. Phys.* 94: 8640
88. Leikin, S. 1991. *J. Chem. Phys.* 95: 5224–29
89. Attard, P., Patey, G. N. 1991. *Phys. Rev. A* 43: 2953–62
90. Helfrich, W. 1978. *Z. Naturforsch. Teil A* 33a: 305–315
91. Helfrich, W., Harbich, W. 1985. *Chem. Scr.* 25: 32–36
92. Selinger, J. V., Bruinsma, R. F. 1991. *Phys. Rev. A* 43: 2910–21
93. Hentschke, R., Herzfeld, J. 1991. *Phys. Rev. A* 44: 1148–1155
94. de Gennes, P.-G., Pincus, P. 1990. *C. R. Acad. Sci.* 310: 697–700
95. de Gennes, P.-G. 1992. In *Mechanics of Swelling: From Clays to Living Cells and Tissues*, ed. T. K. Karalis, NATO ASI Ser. H, Cell Biology, 64: 595–601. Berlin: Springer-Verlag
96. Safinya, C. R., Roux, D., Smith, G. S., Sinha, S., Dimon, P., et al. 1986. *Phys. Rev. Lett.* 57: 2718–21
97. Roux, D., Safinya, C. R. 1988. *J. de Physique* 49: 307–18
98. Podgornik, R., Parsegian, V. A. 1990. *Macromolecules* 23: 2265–69
99. Evans, E., Parsegian, V. A. 1986. *Proc. Natl. Acad. Sci. USA* 83: 7132–36
100. Evans, E., Needham, D. 1987. *J. Phys. Chem.* 91: 4219–28
101. Podgornik, R., Parsegian, V. A. 1992. *Langmuir* 8: 557–62
102. Nilsson, U., Jonsson, B., Wennerstrom, H. 1990. *Faraday Discuss. Chem. Soc.* 90: 107–14
103. Granfeld, M. K., Miklavic, S. J. 1991. *J. Phys. Chem.* 95: 6351–60
104. McIntosh, T. J., Magid, A. D., Simon, S. A. 1987. *Biochemistry* 26: 7325–32
105. Israelachvili, J. N., Wennerstrom, H. 1990. *Langmuir* 6: 873–76
106. Tanford, C. 1980. *The Hydrophobic Effect: Formation of Micelles and Biological Membranes*. New York: Wiley. 233 pp. 2nd ed.
107. Parsegian, V. A., Rand, R. P. 1991. *Langmuir* 7: 1299–303
108. Parsegian, V. A., Rand, R. P. 1992. *Langmuir* 8: 1502
109. Marsh, D. 1989. *Biophys. J.* 55: 1093–1100
110. Marcelja, S., Radic, N. 1976. *Chem. Phys. Lett.* 42: 129–30
111. Landau, L. D., Lifshitz, E. M. 1980. *Statistical Physics, Part I.* 3rd ed. Oxford: Pergamon
112. Kornyshev, A. A., Leikin, S. 1989. *Phys. Rev. A* 40: 6431–37
113. Leikin, S., Kornyshev, A. A. 1991. *Phys. Rev. A* 44: 1156–68
114. Cevc, G. 1991. *J. Chem. Soc. Faraday Trans.* 87: 2733–39
115. Gruen, D. W. R., Marcelja, S. 1983. *J. Chem. Soc. Faraday Trans.* 2 79: 225–42
116. Schiby, D., Ruckenstein, E. 1983. *Chem. Phys. Lett.* 95: 435–38
117. Cevc, G., Marsh, D. 1985. *Biophys. J.* 47: 21–31
118. Cevc, G. 1985. *Chem. Scr.* 25: 97–107
119. Belaya, M., Feigelman, M., Levadny, V. G. 1987. *Langmuir* 3: 648–54
120. Kornyshev, A. A. 1986. *J. Electroanal. Chem.* 204: 79–84
121. Dzhavakhidze, P. G., Kornyshev, A. A., Levadny, V. G. 1986. *Phys. Lett. A* 118: 203–8
122. Dzhavakhidze, P. G., Kornyshev, A. A., Levadny, V. G. 1988. *Nuovo Cimento D* 10: 627–53
123. Kornyshev, A. A. 1985. In *The Chemical Physics of Solvation*, ed. R. R. Dogonadze, E. Kalman, A. A. Kornyshev, J. Ulstrup, Part A, pp. 77–118. Amsterdam: Elsevier
124. Loring, R. F., Mukamel, S. 1987. *J. Chem. Phys.* 87: 1272–83
125. Wei, D., Patey, G. N. 1990. *J. Chem. Phys.* 93: 1399–411
126. Neumann, M. 1986. *Mol. Phys.* 57: 97–121

127. Attard, P., Wei, D., Patey, G. N. 1990. *Chem. Phys. Lett.* 172: 69
128. Fonseca, T. F., Ladanyi, B. M. 1990. *J. Chem. Phys.* 93: 8148–55
129. Kornyshev, A. A., Kossakowski, D. A., Vorotyntsev, M. A. 1991. In *Condensed Matter Physics Aspects of Electrochemistry*, ed. M. P. Tosi, A. A. Kornyshev, pp. 93–109. Singapore: World Scientific
130. Berkowitz, M. L., Raghavan, K. 1993. In *Membrane Electrochemistry*, ed. M. Blank, I. Vodyanoy. Washington, DC: ACS Books. In press
131. Radic, N., Marcelja, S. 1978. *Chem. Phys. Lett.* 55: 377–79
132. Schiby, D., Ruckenstein, E. 1983. *Chem. Phys. Lett.* 100: 277–81
133. Kornyshev, A. A., Ulstrup, J. 1985. *Chem. Scr.* 25: 58–62
134. Kjellander, R., Marcelja, S. 1985. *Chem. Phys. Lett.* 120: 393–96
135. Berkowitz, M. L., Raghavan, K. 1991. *Langmuir* 7: 1042–44
136. Raghavan, K., Reddyi, M. R., Berkowitz, M. L. 1992. *Langmuir* 8: 233–40
137. Bergenstahl, B. A., Stenius, P. 1987. *J. Phys. Chem.* 91: 5944–48
138. Attard, P., Batchelor, M. T. 1988. *Chem. Phys. Lett.* 149: 206–11
139. Ben-Naim, A. 1990. *J. Chem. Phys.* 93: 8196–8210
140. Parsegian, V. A., Rand, R. P., Rau, D. C. 1985. *Chem. Scr.* 25: 28–31
141. Kornyshev, A. A., Ulstrup, J. 1986. *Chem. Phys. Lett.* 126: 74–80
142. Kjaer, A. M., Ulstrup, J. 1987. *Inorg. Chem.* 26: 2052–58
143. Schumaker, G., Sandermann, H. 1976. *Biochim. Biophys. Acta* 448: 642–44
144. Kornyshev, A. A., Kossakowski, D. A., Leikin, S. L. 1992. *J. Chem. Phys.* 97: 6809–20
145. Seddon, J. M., Cevc, G., Kaye, R. D., Marsh, D. 1984. *Biochemistry* 23: 2634–44
146. Mulukutla, S., Shipley, G. G. 1984. *Biochemistry* 23: 2514–19
147. Portis, A., Newton, C., Pangborn, W., Papahadjopolous, D. 1979. *Biochemistry* 18: 780–90
148. Hauser, H., Shipley, G. G. 1984. *Biochemistry* 23: 34–41
149. Feigenson, G. W. 1986. *Biochemistry* 25: 5819–25
150. Coorsen, J. 1988. MS thesis. Brock Univ., St. Catharines, Ontario
151. Saegner, W., Hunter, W. N., Kennard, O. 1986. *Nature* 324: 385–88
152. Cevc, G., Marsh, D. 1987. *Phospholipid Bilayers*. New York: Wiley
153. Cevc, G. 1989. *J. de Physique* 50: 1117–34
154. Gawrisch, K., Parsegian, V. A., Hajduk, D. A, Tate, M. W., Gruner, S. M., et al. 1992. *Biochemistry* 31: 2856–64
155. Guldbrand, L., Jonsson, B., Wennerstrom, H. 1982. *J. Colloid Interface Sci.* 89: 532–41
156. Goldstein, R. E., Leibler, S. 1989. *Phys. Rev. A* 40: 1025–35
157. Podgornik, R. 1989. *Chem. Phys. Lett.* 163: 531–36
158. Zimmerberg, J., Parsegian, V. A. 1986. *Nature* 323: 36–39
159. Zimmerberg, J., Benzanilla, F., Parsegian, V. A. 1990. *Biophys. J.* 57: 1049–64
160. Rayner, M. D., Starkus, J. G., Ruben, P. C., Alicata, D. A. 1992. *Biophys. J.* 61: 96–108
161. Keller, S. L., Bezrukov, S. M., Gruner, S. M., Vodyanoy, I., Parsegian, V. A. 1992. *Biophys. J.* 61: A115
162. Colombo, M. F., Rau, D. C., Parsegian, V. A. 1992. *Science* 256: 655–59
163. Kornblatt, J. A., Hoa, G. H. B. 1990. *Biochemistry* 29: 9370
164. Rand, R. P., Fuller, N. L. 1992. *Biophys. J.* 61: A345